Applied
Organometallic
Chemistry

Received: 29 July 2015 Revised: 16 September 2015 Accepted: 18 October 2015

(wileyonlinelibrary.com) DOI 10.1002/aoc.3405

Synthesis, structural characterization and biological studies of neodymium(III) and samarium(III) complexes with mercaptotriazole Schiff bases

Qurratul Ain, Sarvesh Kumar Pandey, Om Prakash Pandey and Soumitra Kumar Sengupta*

A series of neodymium(III) and samarium(III) complexes of type [Ln(L)Cl(H_2O)$_3$] have been synthesized with Schiff bases (LH_2) derived from 3-(phenyl/substituted phenyl)-4-amino-5-mercapto-1,2,4-triazoles and isatin. The structures of the complexes were established using elemental analysis, molar conductivities, magnetic moments, infrared, NMR (^1H, ^{13}C) and UV–visible spectra, X-ray diffraction and mass spectrometry. The thermal behaviour of these compounds under non-isothermal conditions was investigated using thermogravimetry and differential thermogravimetry. The intermediates obtained at the end of various thermal decomposition steps were identified from elemental analysis and infrared spectral studies. All the ligands and their complexes were also screened for their antibacterial activity against *Staphylococcus aureus* and *Bacillus subtilis* and antifungal activity against *Aspergillus niger*, *Aspergillus flavus* and *Colletotrichum capsici*. The screening results were correlated with the structural features of the compounds. Copyright © 2015 John Wiley & Sons, Ltd.

Additional supporting information may be found in the online version of this article at the publisher's web-site.

Keywords: 1,2,4-triazoles; Schiff bases; neodymium(III); samarium(III); antimicrobial

Introduction

Schiff bases are very accomplished ligands in transition metal as well as inner-transition metal complexes with suitable properties for theoretical and practical applications.[1] Heterocyclic Schiff bases derived from 1,2,4-triazoles have received much attention, particularly in the study of complex formation because they exhibit interesting biological activities. 1,2,4-Triazole moieties have been incorporated into a wide variety of therapeutically interesting drug candidates including anti-inflammatories, central nervous system stimulants, sedatives, anti-anxiety agents and antimicrobial agents.[2,3] There are various known drugs containing 1,2,4-triazole moieties, such as fluconazole, itraconazole, voriconazole,[4,5] triazolam,[6] alprazolam,[7] etizolam,[8] ribavirin,[9] mycobutanil,[10] rizatriptan[11] and fluotrimazole.[12] 1,2,4-Triazole ligands are considered to be good coordinating ligands because they involve both hard nitrogen and soft sulfur atoms in a thioamide group. These ligands have donor groups that coordinate with a wide range of metal ions. The diverse applications are at least in part a consequence of the numerous approaches that are available for the insertion of specific functionalities into the 1,2,4-triazole nucleus.[13–15] However, lanthanide(III) complexes formed with heterocyclic Schiff bases, particularly those containing a 1,2,4-triazole ring system, have received comparatively less attention. Apart from structural diversities and bonding interactions, the multitude of applications of lanthanide complexes makes them an exciting area of coordination chemistry.

Keeping in view the above facts and in continuation of our research on biologically potent molecules, we herein report the synthesis, spectroscopic properties, thermal behaviour and antimicrobial (antibacterial and antifungal) activities of neodymium(III) and samarium (III) complexes with Schiff bases derived from 3-(phenyl/substituted phenyl)-4-amino-5-mercapto-1,2,4-triazole and isatin.

Experimental

Materials and spectral measurements

All reagents were of analytical grade and were used without further purification. Neodymium(III) chloride and samarium(III) chloride were purchased from Merck.

Nitrogen was estimated using the Kjeldahl method and neodymium and samarium were determined gravimetrically as neodymium oxide and samarium oxide. Elemental analysis (C, H and N) was conducted using a Coleman CHN analyser. Melting points were determined with a Buchi 530 apparatus in open capillary tubes. Molar conductance of 10^{-3} M solutions of the complexes in dimethylsulfoxide (DMSO) was recorded with a Hanna EC 215 conductivity meter using 0.01 M KCl water solution as calibrant.

---

* *Correspondence to: Soumitra Kumar Sengupta, Chemistry Department, DDU Gorakhpur University, Gorakhpur – 273009, India.
E-mail: sengupta@hotmail.co.uk*

Chemistry Department, DDU Gorakhpur University, Gorakhpur - 273009, India

Magnetic susceptibility measurements of the complexes in powder form were carried out at room temperature using a Gouy balance. The effective magnetic moments (μ_{eff}) were calculated using the formula

$$\mu_{eff} = 2.238\sqrt{\chi_m \times T} \quad (1)$$

where T is the absolute temperature and χ_m the molar susceptibility obtained after employing diamagnetic corrections. The magnetic moment is usually expressed in units called Bohr magnetons (BM).

Infrared (IR) spectra were recorded with a Matson model 1000 FTIR spectrophotometer using KBr discs. ^{1}H NMR and ^{13}C NMR spectra were recorded with a Jeol AL300 spectrometer using DMSO-d_6 as solvent. Chemical shifts (δ) were measured in parts per million (ppm) relative to an internal standard of Me_4Si. A Hitachi (Japan) model U-2000 spectrophotometer was used to record the electronic spectra. The particle size of the complexes was calculated by analysis of X-ray diffraction patterns, obtained using a powder X-ray diffractometer (Rigaku Geigerflex) with a Cu Kα ($\lambda = 1.54060$ Å) source. Thermogravimetric analyses were conducted from 50 to 830°C at a heating rate of 10°C min^{-1}. The data were obtained using a PerkinElmer Diamond instrument. High-resolution mass spectra were recorded with a Waters Micromass Q-Tof Micro.

General method for synthesis of 3-(phenyl/substituted phenyl)-4-amino-5-mercapto-1,2,4-triazoles

The method used was that of Tomayo.[16] Carbon disulfide (38.4 mmol) was slowly added in a methanolic solution of the appropriate hydrazide (36.5 mmol) and KOH (36.5 mmol) with constant stirring. This solution was stirred further for 2–3 h and left overnight. The mixture was then treated with hydrazine hydrate (36.5 mmol) and refluxed for 4 h. The resulting mixture was cooled and filtered. The filtrate was acidified with dilute HCl to afford the triazoles, which were recrystallized from aqueous ethanol.

Synthesis of Schiff bases

The Schiff bases (LH_2) were prepared by the condensation of 3-(phenyl/substituted phenyl)-4-amino-5-mercapto-1,2,4-triazoles with isatin as reported in the literature.[17–21] The general procedure for synthesis of the Schiff bases is shown in Scheme 1.

Synthesis of Nd(III) and Sm(III) complexes (1–10)

To a solution of appropriate ligand (1 mmol) in ethanol (20 cm^3), the appropriate $LnCl_3 \cdot 6H_2O$ (Ln = Nd, Sm; 1 mmol) in ethanol (10 cm^3) was added and the pH of the reaction mixture was adjusted to *ca* 6.0 using sodium hydroxide solution. The reaction mixture was refluxed for 12–20 h. The product formed was filtered, washed with water followed by ethanol and dried *in vacuo*.

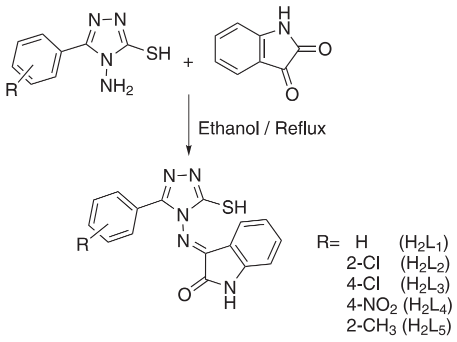

Scheme 1. Synthesis of Schiff bases.

Table 1. Antibacterial and antifungal activities of Schiff bases, Nd(III) and Sm(III) complexes and standards

Compound	Conc. (μg ml^{-1})	Antibacterial activity: zone of inhibition (%)		Antifungal activity: zone of inhibition (%)		
		S. aureus	*B. subtilis*	*A. niger*	*A. flavus*	*C. capsici*
L^1H_2	100	40.4	49.3	52.5	38.5	—
	50	30.5	39.5	41.6	29.3	—
	25	18.0	27.7	30.5	18.1	—
L^2H_2	100	68.5	75.0	80.5	64.5	52.3
	50	57.2	61.0	69.7	53.8	42.8
	25	46.3	50.4	58.2	42.0	30.6
L^3H_2	100	60.0	70.2	72.7	56.7	43.0
	50	50.3	60.1	61.5	45.3	30.3
	25	38.5	46.5	50.0	36.7	22.4
L^4H_2	100	49.4	60.6	61.3	47.6	33.2
	50	38.3	49.7	50.7	38.2	22.8
	25	27.8	35.5	40.4	28.7	15.9
L^5H_2	100	30.4	40.2	45.8	28.5	—
	50	21.3	29.0	33.1	18.0	—
	25	10.4	19.5	25.7	10.4	—
$[Nd(L^1)Cl(H_2O)_3]$	100	58.3	60.8	61.8	46.3	—
	50	36.4	47.5	50.1	35.0	—
	25	25.6	35.6	39.4	26.5	—
$[Nd(L^2)Cl(H_2O)_3]$	100	75.7	86.5	88.3	72.1	60.1
	50	66.2	71.5	77.4	63.3	50.5
	25	55.4	59.8	65.7	52.6	38.3
$[Nd(L^3)Cl(H_2O)_3]$	100	68.5	79.5	80.2	64.2	51.0
	50	55.7	67.3	70.5	52.0	40.2
	25	45.3	53.6	59.5	45.1	28.6
$[Nd(L^4)Cl(H_2O)_3]$	100	57.0	70.1	70.2	55.3	40.0
	50	45.7	57.5	58.0	45.4	29.0
	25	35.2	45.1	47.0	34.4	20.0
$[Nd(L^5)Cl(H_2O)_3]$	100	38.5	48.5	52.1	37.0	—
	50	28.2	38.5	41.3	26.0	—
	25	17.5	27.0	30.5	17.0	—
$[Sm(L^1)Cl(H_2O)_3]$	100	60.5	60.5	60.5	46.7	—
	50	35.8	47.7	51.0	35.4	—
	25	26.2	34.8	38.8	25.5	—
$[Sm(L^2)Cl(H_2O)_3]$	100	75.0	86.2	87.2	72.3	59.7
	50	65.7	70.9	75.8	62.7	51.2
	25	56.2	58.9	64.5	51.9	38.3
$[Sm(L^3)Cl(H_2O)_3]$	100	68.8	78.5	78.8	64.0	50.6
	50	56.5	66.7	69.4	52.7	41.1
	25	45.0	53.5	59.0	40.7	28.5
$[Sm(L^4)Cl(H_2O)_3]$	100	57.1	70.4	70.6	55.1	40.5
	50	46.0	58.8	58.8	45.0	29.7
	25	35.9	45.4	47.3	34.7	20.3
$[Sm(L^5)Cl(H_2O)_3]$	100	39.6	49.7	52.3	37.4	—
	50	28.5	38.1	41.0	26.2	—
	25	17.3	27.5	30.2	17.6	—
Standard	100	100	100	100	100	100
	50	100	100	100	100	100
	25	100	100	100	100	100

In vitro antibacterial and antifungal activity

The synthesized Schiff bases and complexes were screened *in vitro* for their antimicrobial activity against two bacteria, namely *Staphylococcus aureus* and *Bacillus subtilis*, and three fungi, namely *Aspergillus niger*, *Aspergillus flavus* and *Colletotricum capsici*, using reported methods.[22] A stock solution (1 mg ml^{-1}) of the test chemical was prepared by dissolving 10 mg of the test compound in 10 ml of *N*,*N*-dimethylformamide (DMF) solvent. The stock solution was suitably diluted with sterilized distilled water to get dilutions of 100, 50 and 25 μg ml^{-1}. Control for each dilution was prepared by diluting 10 ml of solvent instead of stock solution with sterilized distilled water.

The bacteria were subcultured in agar medium. Petri dishes were incubated for 24 h at 37°C. Standard antibacterial drug (gentamicin) was also screened under similar conditions for comparison. The fungi were subcultured in potato dextrose agar medium. Standard antifungal drug (fluconazole) was used for comparison. Petri dishes were incubated for 48 h at 37°C. Wells were dug in the agar media using a sterile metallic borer. Activity was determined by measuring the diameter (mm) of the zone showing complete inhibition (Table 1). Growth inhibition was compared with that of the standard drugs. The percentage inhibition of the growth of the test organism was calculated using the following formula:

$$\text{Inhibition}\ (\%) = 100 \times \frac{C_\mathrm{d} - T_\mathrm{d}}{C_\mathrm{d}} \qquad (2)$$

where C_d is the colony diameter of the control and T_d the colony diameter of the treated set. Each set was kept in triplicate.

Results and discussion

The Schiff bases are soluble in DMF and DMSO. All the neodymium (III) and samarium(III) complexes are stable at room temperature and are non-hygroscopic. The results of the elemental analyses are summarized in Table 2. The molar conductance values in DMF are in the range 9–12 Ω^{-1} cm^2 mol^{-1} (Table 2), indicating the non-electrolytic behaviour of the complexes in solution.

IR spectra

The IR spectral data for all complexes are summarized in Table 3. Organic compounds having a thioamide group (H–N–C=S) give rise to four thioamide bands (*ca* 1520, *ca* 1300–1400, 1000 and 700–850 cm^{-1}) in IR spectra. These bands have contributions from δ(C–H) + δ(N–H), ν(C=S) + ν(C=N) + δ(C–H) and ν(C–N). For the ligands under investigation here, these bands appear at 1510–1530, 1280–1320, 1040–1060 and 780–820 cm^{-1}. The bands are expected to be affected differently by different modes of coordination. It has been suggested that the coordination of amido nitrogen is accompanied by a small increase in the thioamide I band. Coordination through the thioketosulfur causes a decrease in the frequency of the thioamide IV band. However, in the complexes under investigation, all thioamide bands disappear indicating that mixing of ν(C–N), δ(N–H) and ν(C=S) vibrations may be absent. In addition, a weak band at 2560–2585 cm^{-1} in the spectra of the ligands (in solution) due to the –SH group vibration further suggests the thione–thiol tautomerism. However, in the spectra of

Table 2. Elemental analyses of neodymium(III) and samarium(III) complexes

Compound	Empirical formula	Yield (%)	M.p. (°C)	C (%)	H (%)	N (%)	Ln (%)	μ_eff (BM)	Molar conductance (Ω^{-1} cm^2 mol^{-1})
				Found (calcd)	Found (calcd)	Found (calcd)	Found (calcd)		
1	$C_{16}H_{15}N_5SO_4ClNd$	68	160	34.50 (34.74)	2.56 (2.71)	12.49 (12.66)	26.05 (26.09)	3.55	12.0
2	$C_{16}H_{14}N_5SO_4Cl_2Nd$	58	175	32.46 (32.69)	2.13 (2.38)	11.75 (11.92)	24.32 (24.56)	3.58	10.6
3	$C_{16}H_{14}N_5SO_4Cl_2Nd$	70	230	32.47 (32.69)	2.11 (2.38)	11.78 (11.92)	24.34 (24.56)	3.40	10.4
4	$C_{16}H_{14}N_6SO_6ClNd$	75	190	32.05 (32.12)	2.25 (2.34)	14.00 (14.05)	24.06 (24.13)	3.50	9.8
5	$C_{17}H_{17}N_5SO_5ClNd$	65	195	35.00 (35.01)	2.75 (2.92)	11.97 (12.01)	24.53 (24.75)	3.45	12.0
6	$C_{16}H_{15}N_5SO_4ClSm$	65	170	34.16 (34.36)	2.45 (2.68)	12.41 (12.53)	26.78 (26.90)	1.45	10.5
7	$C_{16}H_{14}N_5SO_4Cl_2Sm$	60	182	32.19 (32.36)	2.22 (2.36)	11.55 (11.79)	25.28 (25.34)	1.40	11.7
8	$C_{16}H_{14}N_5SO_4Cl_2Sm$	74	220	32.20 (32.36)	2.23 (2.36)	11.58 (11.79)	25.21 (25.34)	1.45	11.1
9	$C_{16}H_{14}N_6SO_6ClSm$	72	185	31.57 (31.79)	2.18 (2.32)	13.80 (13.91)	24.70 (24.89)	1.50	9.0
10	$C_{17}H_{17}N_5SO_5ClSm$	69	210	34.45 (34.64)	2.68 (2.89)	11.70 (11.89)	25.32 (25.53)	1.42	10.5

Table 3. Important IR frequencies (cm^{-1}) of neodymium(III) and samarium(III) complexes

Compound	Formula	ν(OH)	ν(C–O)	ν(C=N)	ν(Ln–N)	ν(Ln–S)	ν(Ln–O)
1	$C_{16}H_{15}N_5SO_4ClNd$	3424	1240	1605	415	390	510
2	$C_{16}H_{14}N_5SO_4Cl_2Nd$	3460	1245	1610	425	380	515
3	$C_{16}H_{14}N_5SO_4Cl_2Nd$	3495	1245	1600	420	388	520
4	$C_{16}H_{14}N_6SO_6ClNd$	3440	1235	1605	435	378	510
5	$C_{17}H_{17}N_5SO_5ClNd$	3450	1238	1610	440	390	510
6	$C_{16}H_{15}N_5SO_4ClSm$	3420	1232	1605	430	375	500
7	$C_{16}H_{14}N_5SO_4Cl_2Sm$	3475	1245	1610	445	385	500
8	$C_{16}H_{14}N_5SO_4Cl_2Sm$	3485	1240	1600	415	390	500
9	$C_{16}H_{14}N_6SO_6ClSm$	3448	1235	1610	428	385	515
10	$C_{17}H_{17}N_5SO_5ClSm$	3445	1230	1615	420	385	500

the complexes these bands disappear, indicating the coordination through sulfur after deprotonation. The IR spectra of the complexes show a band at 620 cm^{-1} which is due to conversion of C=S to C–S–. The ν(Ln–S) vibration appears at 375–390 cm^{-1}.

The bands observed around 1620–1640, 1570–1590 and 1500–1550 cm^{-1} in the spectra of the ligands may be assigned to ν(C=N), ν(C=N) (triazole ring) and ν(C=C) (phenyl) vibrations, respectively. Strong vibrations in the region 1550–1600 cm^{-1} are usually associated with phenyl and C=N groups and it is normally not possible to identify such bands with particular C=C or C=N linkage. However, a stringent assignment of C=N group can be made by comparing the spectrum of the parent mercaptotriazole containing N–NH$_2$ group with that of the ligands in which N–NH$_2$ group is replaced by N–N=CH group. Following this method, the strong band observed at 1620–1640 cm^{-1} is assigned to the ν(C=N) vibration. The spectra of the complexes show the shifting of this band to lower frequency (*ca* 20 cm^{-1}) indicating the coordination of the azomethine nitrogen to the metal atom. The bands observed at 415–445 cm^{-1} may be assigned to ν(Ln–N).

The IR spectra of the ligands LH$_2$ show a broad band at about 3320–3335 cm^{-1} due to ν(–OH) (in solution), which disappears in the spectra of the corresponding complexes indicating the deprotonation of O–H group.[23,24] The ν(Ln–O) vibration band appears at 500–520 cm^{-1}. The presence of coordinated water molecules in the complexes is indicated by a broad band in the region 3400–3500 cm^{-1}.

^{1}H NMR spectra

The proton magnetic resonance spectra of neodymium(III) complexes were recorded in DMSO-d_6. Assignments of chemical shifts for protons in various environments are given in Table 4. The ^{1}H NMR spectra (in DMSO-d_6) of Schiff bases exhibit a singlet at 8.5 ppm due to thiol proton (s, 1H, –SH) and 10.5 ppm assigned to enolic proton (s, 1H, –OH).[25,26] These signals disappear in the spectra of the neodymium(III) complexes indicating deprotonation of thiol and enolic groups. The chemical shift covering a range of 7.2–8.3 ppm in the spectra of Schiff bases and their neodymium (III) complexes is due to benzene ring (attached to triazole nucleus and isatin) protons. Neodymium(III) complexes show a new signal at 5.4 ppm due to H$_2$O (s, 6H, –OH).

^{13}C NMR spectra

The ^{13}C NMR spectra of neodymium(III) complexes were recorded in DMSO-d_6 (Table 5). In the spectra of the Schiff bases, the signals are observed in the region 161.8–163.0 ppm are due to azomethine carbon (C=N, 1C). This signal is shifted downfield in the spectra of the complexes due to the coordination through azomethine nitrogen to the central metal ion. In the spectra of all Schiff bases and their corresponding neodymium(III) complexes, the peaks observed at 158.5 and 152.0 ppm are assignable to triazole ring carbons (2C). For the benzene ring, a number of signals appear at 123.4–149.5 ppm (12C). In the spectra of Schiff bases, the signal at 159.2 ppm may be assigned to C–O (1C) of isatin moiety which is shifted downfield in the spectra of the complexes. This shifting is due to the decrease of the electron density in the enolate anions on coordination to the lanthanide atom moiety during complexation.

Magnetic moments and electronic spectra

The magnetic moment values for the neodymium(III) and samarium (III) complexes lie in the range 3.40–3.58 and 1.40–1.50 BM,

Table 4. ^{1}H NMR data for neodymium(III) complexes

Compound	Formula	Aromatic protons (δ, ppm)	H$_2$O protons (δ, ppm)	–CH$_3$ protons (δ, ppm)
1	$C_{16}H_{15}N_5SO_4ClNd$	7.31–7.50 (4H, m, Ar–H); 7.62–8.30 (5H, m, Ar–H)	5.40 (6H, s)	—
2	$C_{16}H_{14}N_5SO_4Cl_2Nd$	7.25–7.58 (4H, m, Ar–H); 7.74–7.85 (4H, m, Ar–H)	5.42 (6H, s)	—
3	$C_{16}H_{14}N_5SO_4Cl_2Nd$	7.35–7.61 (4H, m, Ar–H); 7.66 (d, 2H, *J* = 7.8 Hz, Ar–H); 8.20 (d, 2H, *J* = 7.8 Hz, Ar–H)	5.45 (6H, s)	—
4	$C_{16}H_{14}N_6SO_6ClNd$	7.35–7.50 (4H, m, Ar–H); 8.26 (d,-2H, *J* = 7.8 Hz, Ar–H); 8.30 (d, 2H, *J* = 7.8 Hz, Ar–H)	5.48 (6H, s)	—
5	$C_{17}H_{17}N_5SO_5ClNd$	7.29–7.58 (4H, m, Ar–H); 7.60–7.89 (4H, m, Ar–H)	5.40 (6H, s)	2.37 (3H, s)

Table 5. ^{13}C NMR data for neodymium(III) complexes

Compound	Formula	Phenyl carbons (δ, ppm)^a	Triazole carbons (δ, ppm)	–C=N (δ, ppm)	–CH$_3$ (δ, ppm)	C–O (δ, ppm)
1	$C_{16}H_{15}N_5SO_4ClNd$	123.5, 126.8, 127.0, 127.5, (2C, Ar), 129.6 (2C, Ar), 130.2 (Ar), 130.9 (Ar), 131.8, 132.2, 148.0 (–O–C=N–)	152.0, 158.5 (2C)	167.7 (1C)	—	159.2 (1C)
2	$C_{16}H_{14}N_5SO_4Cl_2Nd$	123.4, 126.5, 127.3, 127.9 (Ar), 128.9 (Ar), 129.2 (Ar), 129.8 (Ar), 130.9 (Ar), 131.5, 132.0, 132.9 (Ar), 148.5 (–O–C=N–)	152.5, 158.6 (2C)	167.8 (1C)	—	159.6 (1C)
3	$C_{16}H_{14}N_5SO_4Cl_2Nd$	124.2, 126.9, 127.8, 128.6, (2C, Ar), 130.6 (Ar),131.0 (Ar), 131.7, 132.6, 133.5 (2C, Ar), 148.7 (–O–C=N–)	152.8, 158.5 (2C)	167.8 (1C)	—	159.5 (1C)
4	$C_{16}H_{14}N_6SO_6ClNd$	123.9, 126.6, 126.9, 127.0 (2C, Ar), 128.7 (2C, Ar), 130.2 (Ar), 131.8, 132.2, 145.3 (Ar), 148.7 (–O–C=N–)	152.5, 158.5 (2C)	167.3 (1C)	—	159.0 (1C)
5	$C_{17}H_{17}N_5SO_5ClNd$	124.5, 126.8, 127.0, 127.7 (Ar), 127.9 (Ar), 129.6 (Ar), 130.5 (Ar), 131.2 (Ar), 132.7, 133.6, 135.2 (Ar), 149.5 (–O–C=N–)	152.2, 158.7 (2C)	167.5 (1C)	19.5 (1C)	159.1 (1C)

[a] Ar = phenyl ring attached to triazole ring.

respectively (Table 2). These values show little deviation from van Vleck values and those of hydrated sulfates.

Tripositive neodymium and samarium ions have the outer configuration $4f^35s^25p^6$ and $4f^55s^25p^6$, respectively, and follow the Russell–Saunders L, S, J coupling scheme but with a certain amount of configuration interaction. The 5 s and 5p subshells have a radial dispersion which is greater than that of the 4f electrons, and hence shield the latter from the effect of coordinated ligands to a very large extent, but not completely.[27] Thus, the electronic spectra of neodymium(III) and samarium(III) can be considered as derived from the spectra of gaseous ions by a fairly small perturbation. This perturbation may be of two general types. The first is a general nephelauxetic effect owing to a drift of ligand or 5 s, 5p electron density into the metal ion, slightly expanding the 4f subshell and reducing the 4f–4f interactions. The second is a crystal field splitting effect, which removes the degeneracy of the free ion levels, and which can be represented with fair success by a point negative charge model having the appropriate molecular symmetry.[28–30]

The f^3 configuration of a free neodymium(III) ion involves 41 energy levels. The absorption spectra of neodymium(III) complexes (Fig. 1) in crystal form and solution contain many bands due to transitions from the ground level $^4I_{9/2}$ to excited levels of the f^3 configuration. The absorption spectra of neodymium(III) complexes derived from isatin show bands around 12 450, 12 800–12 900, 13 000–13 600, 13 800, 17 510, 19 500, 20 500–21 500 and 23 000–23 250 cm^{-1} corresponding to the transitions from the ground level $^4I_{9/2}$ to excited levels $^4F_{5/2}$, $^2H_{9/2}$, $^4F_{7/2}$, $^2S_{3/2}$, $^2G_{7/2}$, $^4G_{9/2}$, $^2G_{9/2}$ and $^2P_{1/2}$, respectively. The f–f transitions are weakly allowed due to some mixing of the excited state of the opposite parity into the ground state and a marked enhancement in the intensity of bands upon complexation is observed. This is due to an increase in the configuration interaction upon complexation.

The f^5 configuration of samarium(III) ion contains 198 levels with various J. The ground state level is $^6H_{5/2}$. The absorption spectra of samarium(III) complexes (Fig. 2) show bands due to transitions from the ground level $^6H_{5/2}$ to excited energy levels $^4G_{5/2}$, $^4F_{3/2}$, $^4G_{7/2}$, $^4I_{9/2}$, $^4I_{13/2}$, $^6P_{5/2}$ and $^4F_{9/2}$. All the transitions corresponds to bands at 17 200–17 350, 18 510, 20 000, 20 500–20 600, 21 510, 23 600–23 900, 25 000–25 300 cm^{-1}, respectively.

A general feature in the spectra of lanthanides is a shift of absorption bands towards lower energy on complex formation, i.e. the nephelauxetic effect.[31] This effect is quantitatively described by a naphelauxetic parameter ($\overline{\beta}$) equal to the ratio of the interelectronic repulsion parameter (either Slater's integrals F_k or Racah's parameter E^k) in the complex and in the free ion:

$$\overline{\beta} = \frac{(F_k)_{\text{complex}}}{(F_k)_{\text{free-ion}}} \text{ or } \overline{\beta} = \frac{(E^k)_{\text{complex}}}{(E^k)_{\text{free-ion}}} \tag{3}$$

As the naphelauxetic effect value $(1-\overline{\beta})$ is small in lanthanide complexes, it can, to a fairly good approximation, be defined from the ratio of the wavenumbers of f–f transitions in the spectra of the complex and the free ion:

$$\overline{\beta} \approx \frac{V_{\text{complex}}}{V_{\text{free-ion}}} \tag{4}$$

Since, in general, the energy levels in the lanthanide free ions are unknown, the relative nephelauxetic effect values $\overline{\beta}$ are usually determined from experimental data using the spectra of the lanthanide aqua ions as standards:

$$\overline{\beta} = \frac{1}{n}\sum_{n=1}^{n}\frac{V_{\text{complex}}}{V_{\text{aqua}}} \tag{5}$$

From the mean $\overline{\beta}$ values, Sinha's covalency parameter (δ) and bonding parameter ($b^{1/2}$) are calculated using the following formulas:

$$\delta = \frac{1-\overline{\beta}}{\overline{\beta}} \times 100 \text{ and } b^{1/2} = \left[\frac{1-\overline{\beta}}{2}\right]^{1/2} \tag{6}$$

These parameters measure the amount of 4f–ligand mixing, i.e. covalency.

The values of the parameters $\overline{\beta}$, δ and $b^{1/2}$ for the complexes are given in Table 6. The values of $\overline{\beta}$ being less than unity and the positive values of δ and $b^{1/2}$ support the partial covalent nature of bonding between metal and ligand.

Thermal studies

The thermal stabilities of the neodymium and samarium complexes were examined using the thermogravimetry (TG) and differential thermogravimetry (DTG) techniques in the temperature range 50–830°C at a heating rate of 10°C min^{-1}. The complexes decompose via intermediates to give the respective metal oxide.[32,33] For all complexes, two steps are apparent in the TG–DTG curves (Fig. 3). The first step corresponds to the loss of all water molecules in the temperature range 165–195°C, accompanied by an endothermic effect. Higher temperature of this stage

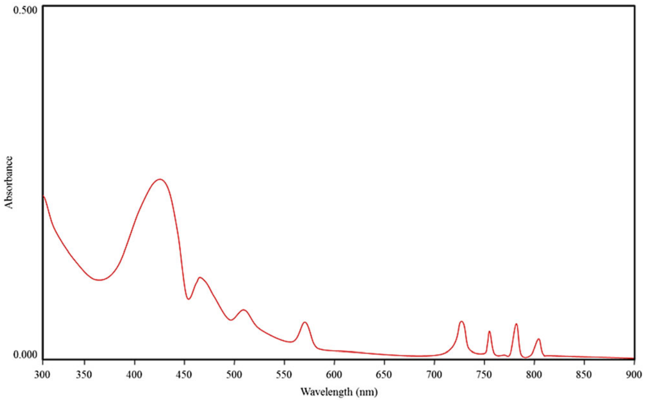

Figure 1. Electronic spectrum of [Nd(L^1)Cl(H_2O)$_3$].

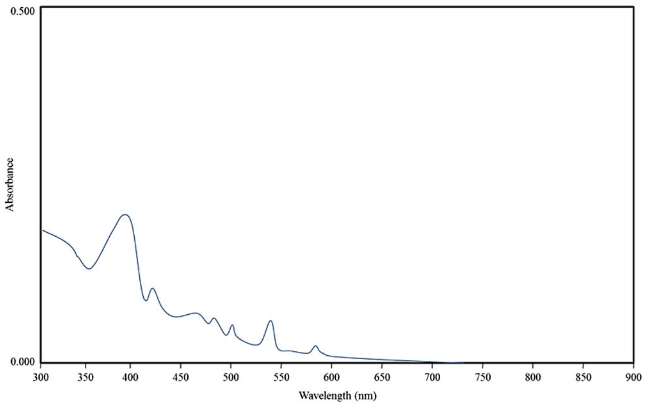

Figure 2. Electronic spectrum of [Sm(L^1)Cl(H_2O)$_3$].

Table 6. Electronic spectral parameters of neodymium(III) and samarium (III) complexes

Compound	Formula	$\overline{\beta}$	δ	$b^{1/2}$
1	$C_{16}H_{15}N_5SO_4ClNd$	0.9868	1.3377	0.0812
2	$C_{16}H_{14}N_5SO_4Cl_2Nd$	0.9870	1.3171	0.0806
3	$C_{16}H_{14}N_5SO_4Cl_2Nd$	0.9860	1.4199	0.0837
4	$C_{16}H_{14}N_6SO_6ClNd$	0.9858	1.4404	0.0843
5	$C_{17}H_{17}N_5SO_5ClNd$	0.9874	1.2761	0.0794
6	$C_{16}H_{15}N_5SO_4ClSm$	0.9792	2.1242	0.1019
7	$C_{16}H_{14}N_5SO_4Cl_2Sm$	0.9793	2.1138	0.1017
8	$C_{16}H_{14}N_5SO_4Cl_2Sm$	0.9799	2.0512	0.1002
9	$C_{16}H_{14}N_6SO_6ClSm$	0.9795	2.0929	0.1012
10	$C_{17}H_{17}N_5SO_5ClSm$	0.9788	2.0616	0.1029

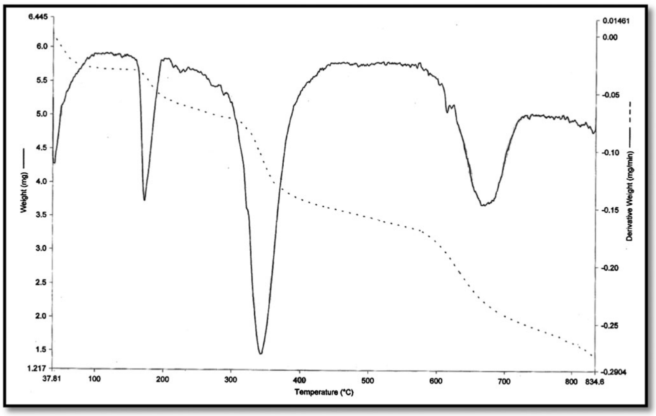

Figure 3. TG–DTG curves of [Nd(L^1)Cl(H$_2$O)$_3$].

suggests a stronger association of complex molecule through intermolecular hydrogen bonding between coordinated water and bonded ligands. The second stage corresponds to the decomposition of the anhydrous complexes to the oxides and is accompanied by a strong exothermic effect with two peaks in the temperature range 345–670°C. The final products of the decomposition of the lanthanide complexes are oxides: ½Nd_2O_3 and ½Sm_2O_3.

X-ray diffraction

Our efforts to prepare single crystals of these complexes were unsuccessful due to the high molecular mass of the metal ions involved. Therefore, powder X-ray diffraction patterns were recorded. Powder X-ray diffraction is a rapid analytical technique. This technique is based on constructive interference of monochromatic X-rays and a crystalline sample.[34,35] These X-rays are generated by a cathode ray tube, filtered to produce monochromatic radiation to concentrate and directed towards the sample.

The powder X-ray diffraction pattern of one representative complex, i.e. [Sm(L^1)Cl(H$_2$O)$_3$], is shown in Fig. 4. The peak broadening at lower angle is significant for the calculation of particle size. Therefore the size of the particles was calculated using the Debye–Scherrer formula:

$$D = 0.94\lambda/\beta \cos \theta \tag{7}$$

where D is the size of the particle, λ is the wavelength of X-rays, β (in rad) is the full width at half maximum after correcting the instrument

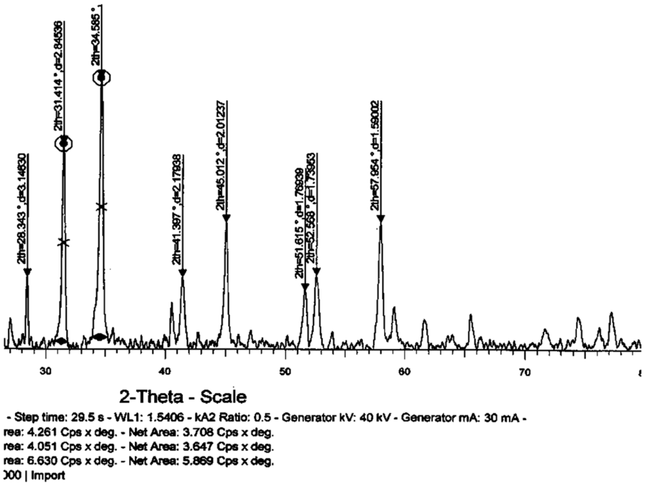

Figure 4. Powder X-ray diffraction pattern of [Sm(L^1)Cl(H$_2$O)$_3$].

peak broadening and θ is the Bragg angle. The size of the particles is found to be in the range 16–28 nm which falls in the nanoscale range.

Pharmacology results

All the synthesized Schiff bases and their corresponding neodymium(III) and samarium(III) complexes were screened *in vitro* for their antimicrobial activity against two bacteria and three fungi. The antimicrobial results are summarized in Table 1. All the complexes possess high antibacterial activity against Gram-positive (*B. subtilis*) bacteria and antifungal activity against *A. flavus*. Complexes [Nd(L^2)Cl(H$_2$O)$_3$], [Nd(L^3)Cl(H$_2$O)$_3$] and [Nd(L^4)Cl(H$_2$O)$_3$] show zones of inhibition of 86.5, 79.5 and 70.0% at 100 µg ml^{-1} against *B. subtilis* which are quite good. The same complexes show good zones of inhibition against *A. flavus*: 86.2, 78.5 and 70.4%, respectively. The antimicrobial studies show that the activity of the ligands increases on coordination with metal ion, i.e. the metal complexes are more active than the free organic ligands. This pronounced increase in activity may be due to the formation of a chelate, a less polar form of the metalloelement, which thereby increases the lipophilic character. The increased lipophilic character of the chelate favours the interaction of these complexes with cell constituents, resulting in interference with normal cell processes. According to Overton's concept of cell permeability, the lipid membrane that surrounds a cell favours the passage of only lipid-soluble materials so that liposolubility is an important factor that controls antimicrobial activity.[36] The widespread interaction of metal ions with cellular components is owing to the fact that lipids and polysaccharides are some important constituents of cell walls and membranes, which are preferred for metal ion interaction. In addition to this, cell walls also contain several aminophosphates and carbonyl and cysteinyl ligands, which maintain the integrity of the membrane by acting as a diffusion barrier and also provide suitable sites for binding. If the geometry and charge distribution around a molecule are incompatible with the geometry and charge distribution around the pores of a cell wall, penetration through the wall by the toxic agent cannot take place and this will prevent a toxic reaction within the pores.[37] Chelation is not the only criterion for antimicrobial activity. The nature of the metal ion and ligand, the coordinating sites, the geometry of the complex, the concentration, the hydrophilicity, the lipophilicity and the presence of co-ligands also influence the activity. In addition to this, steric and pharmacokinetic factors also play decisive roles in deciding the potency of an antimicrobial agent.

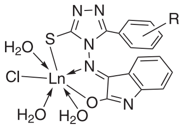

Figure 5. Tentative structure of the complexes.

Mass spectrometry

High-resolution mass spectra were recorded, and, within acceptable limits, the benefits of mass spectrometry in the study of organometallic chemistry are that investigation of molecules and complexes in the gas phase allows determination of the intrinsic properties without interference from solvent or counter ion. TOF-MS spectra of representative complexes show peaks at (*m/z*) 610.9641 and 600.9453, assignable to $[M+NH_3]^+$ (Figs S5 and S6 of the supporting information), and various other peaks corresponding to the fragmentation of degraded species. The patterns of peaks give a clear impression of the successive degradation of the target compound with the series of peaks corresponding to the various fragments with different intensities. The intensity detected for a particular peak is directly related to the stability of degraded fragments. These peaks corresponding to the fragments are observed to confirm the molecular formula of the selected complexes. HRMS (*m/z*): $[M+NH_3]^+$ calcd for $C_{16}H_{14}Cl_2N_5O_4SNd$, 600.9486; found, 600.9453; $[M+NH_3]^+$ calcd for $C_{16}H_{14}Cl_2N_5O_4SSm$, 610.9606; found, 610.9641.

Conclusions

The synthesized 3-(phenyl/substituted phenyl)-4-amino-5-mercapto-1,2,4-triazoles act as tridentate Schiff bases. The metals are coordinated to thiol sulfur, azomethine nitrogen and phenolic oxygen atoms. The analytical, IR, NMR and electronic spectral, magnetic, thermal and X-ray studies confirm the bonding of Schiff bases to metal ions. All Schiff bases and complexes are found to potentially active towards all microbial strains investigated.

All these observation put together lead us to propose a structure for the complexes, as shown in Fig. 5).

Acknowledgements

The authors are grateful to SAIF, Chandigarh, STIC Cochin for providing spectral data, and University Grants Commission (UGC) for financial support. The authors are also grateful to Head, Chemistry Department, DDU Gorakhpur University for providing necessary facilities.

References

[1] H. Gadegoni, S. Manda, *Chin. Chem. Lett.* **2013**, *24*, 127.
[2] a T. Plech, J. J. Luszczki, M. Wujec, J. Flieger, M. Pizo, *Eur. J. Med. Chem.* **2013**, *60*, 208; b S. K. Pandey, A. Singh, A. Singh, Nizamuddin Khan, *Eur. J. Med. Chem.* **2009**, *44*, 1188.
[3] a M. R. Aouad, M. Messali, N. Rezki, A. A. S. Ali, A. Lesimple, *Acta Pharm.* **2015**, *65*, 117; b S. K. Pandey, A. Ahmad, O. P. Pandey, Nizamuddin Khan, *J. Heterocycl. Chem.* **2014**, *51*, 1233.
[4] J. Haber, *Cas. Lek. Cesk.* **2001**, *140*, 596.
[5] A. M. Vijesh, A. M. Isloor, P. Shetty, S. Sundershan, H. K. Fun, *Eur. J. Med. Chem.* **2013**, *62*, 410.
[6] A. Brucato, A. Copoola, S. Gianguzza, P. M. Provenzano, *Bull. Soc. Ital. Sper.* **1978**, *54*, 1051.
[7] M. Zareef, R. Iqbal, N. G. De Dominguez, J. Rodrigues, J. H. Zaidi, M. Arfan, C. T. Supuran, *J. Enzyme Inhib. Med. Chem.* **2007**, *22*, 301.
[8] J. Patole, D. Shingnapurkar, S. Padhye, C. Ratledge, *Bioorg. Med. Chem. Lett.* **2006**, *16*, 1514.
[9] R. W. Sidwell, L. B. Allen, J. H. Hoffman, J. T. Witkowsti, L. N. Simon, *Proc. Soc. Exp. Biol. Med.* **1975**, *148*, 854.
[10] Y. J. Mange, A. M. Isloor, S. Malladi, S. Isloor, H. K. Fun, *Arabian J. Chem.* **2013**, *6*, 177.
[11] S. V. Bhandari, K. G. Bothara, M. K. Raut, A. A. Patil, A. P. Sarkate, V. J. Mokale, *Bioorg. Med. Chem.* **2008**, *16*, 1822.
[12] U. V. Kamble, S. A. Patil, P. S. Badami, *J. Inc. Phenom. Macrocycl. Chem.* **2010**, *68*, 347.
[13] a H. A. Burch, W. O. Smith, *J. Med. Chem.* **1996**, *9*, 405; b H. Wang, M. Lee, Z. Peng, B. Blázquez, E. Lastochkin, M. Kumarasiri, R. Bouley, M. Chang, S. Mobashery, *J. Med. Chem.* **2015**, *58*, 4194.
[14] M. G. Mamolo, D. Zampieri, V. Falagiani, *Arkivoc* **2004**, *5*, 231.
[15] A. M. Isloor, B. Kalluraya, P. Shetty, *Eur. J. Med. Chem.* **2009**, *44*, 3784.
[16] S. K. Pandey, O. P. Pandey, S. K. Sengupta, *Appl. Organometal. Chem.* **2014**, *28*, 681–687.
[17] R. W. Sabins, *J. Sulfur Chem.* **1994**, *16*, 1.
[18] M. Koparir, C. Orek, A. E. Parlak, A. Soylemez, P. Koparir, M. Karatepe, S. D. Dastan, *Eur. J. Med. Chem.* **2013**, *63*, 340.
[19] F. P. Invidiata, G. Furná, I. Lampronti, D. Simoni, *J. Heterocycl. Chem.* **2009**, *34*, 1255.
[20] R. M. A. Rahman, K. O. A. Footy, F. M. Aqlan, *Int. J. Chem. Tech. Res.* **2011**, *3*, 423.
[21] H. K. Fun, C. K. Quah, A. M. Vijesh, S. Malladi, A. M. Isloor, *Acta Crystallogr.* **2010**, *66*, 29.
[22] a A. K. Sadana, Y. Miraza, K. R. Aneja, O. Prakash, *Eur. J. Med. Chem.* **2003**, *38*, 533; b D. Greenwood, R. Slack, J. Peutherer (Eds), *Medical Microbiology. A Guide to Microbial Infections: Pathogenesis, Immunity, Laboratory Diagnosis and Control*, 15th ed, Churchill Livingstone, Edinburgh, **1997**.
[23] G. Singh, P. A. Singh, K. Singh, D. P. Singh, R. N. Handa, S. N. Dubey, *Proc. Natl Acad. Sci. Ind.* **2002**, *72A*, 87.
[24] P. R. Shukla, V. K. Singh, A. M. Jaiswal, J. Narain, *J. Indian Chem. Soc.* **1983**, *60*, 321.
[25] S. A. Patil, M. Manjunatha, A. D. Kulkarni, P. S. Badami, *Complex. Met.* **2014**, *1*, 128.
[26] S. A. Patil, B. M. Badiger, S. M. Kudari, V. H. Kulkarni, *Transit. Met. Chem.* **1983**, *8*, 238.
[27] B. Huidrom, N. R. Devi, T. D. Singh, N. R. Singh, *Spectrochim. Acta A* **2012**, *85*, 127.
[28] F. J. Caires, A. C. Gigante, D. J. C. Gomes, O. T. Filho, M. Ionashiro, *Thermochim. Acta* **2013**, *569*, 8.
[29] J. P. Mehta, P. N. Bhatt, S. N. Mishra, *J. Rare Earths* **2006**, *24*, 648.
[30] K. Gopalakrishnan, M. Kuttappan, P. E. Kuppanagounder, *Transit. Met. Chem.* **2004**, *29*, 90.
[31] D. E. Henrie, G. R. Choppin, *J. Chem. Phys.* **1968**, *49*, 477.
[32] X. U. Dongfang, M. A. Shuzhi, D. U. Guangying, H. E. Qizhuang, S. Dazhi, *J. Rare Earths* **2008**, *26*, 643.
[33] U. P. Singh, R. Kumar, *J. Mol. Struct.* **2007**, *837*, 214.
[34] R. Kumar, U. P. Singh, *J. Mol. Struct.* **2008**, *875*, 427.
[35] C. J. Athira, Y. Sindhu, M. S. Sujamol, K. Mohanan, *J. Serb. Chem. Soc.* **2011**, *76*, 249.
[36] G. B. Bagihalli, P. G. Avaji, S. A. Patil, P. S. Badami, *Eur. J. Med. Chem.* **2008**, *43*, 2639.
[37] B. N. Meyer, N. R. Ferrigni, J. E. Putnam, L. B. Jacobsen, D. E. Nichols, J. L. McLaughlin, *Planta Med.* **1982**, *45*, 31.

Supporting information

Additional supporting information may be found in the online version of this article at the publisher's website.